Coupling Non-Conforming Discrete Models with Lower-Dimensional Entities

Danczyk, J. (<u>irdanczyk@wisc.edu</u>) Suresh, K. (<u>suresh@engr.wisc.edu</u>)
University of Wisconsin – Madison
1513 University Ave.
Madison, WI 53706

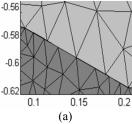
Introduction

In structural mechanics, large scale simulations often exceed the capabilities of a single computer. The underlying spatial domain is therefore partitioned into multiple sub-domains for parallel computation [1, 2]. This partitioning of the spatial domain can be across components of an assembly or an arbitrary interface within a single part. In both cases, the two sides are numerically 'welded' during the analysis.

While the interface geometry, typically defined via computer-aided design (CAD) models, is unique, the discretization, or meshing, procedure will produce a discrete model/mesh that does not necessarily: 1. conform to the CAD model, or 2. conform to the adjoining discrete model. This is typically the case when the interface is a curved surface. Thus the four possible outcomes are:

- 1. *Meshes conform to CAD and to each other*. This case is easily handled since both the CAD models and mesh models conform.
- 2. Meshes don't conform to CAD but conform to each other. Again, this case is easy to handle as the meshes conform.
- 3. Meshes conform to CAD but not to each other. This is illustrated in Figure 1a, and is the classic case of "non-conforming" or "non-matching" grids that is typically addressed by the Mortar Element Method [3-6] (MEM) amongst others [7-12].
- 4. *Meshes don't conform to CAD and don't conform to each other*. This is illustrated by Figure 1b, and is of primary concern in this paper.

While case (4) above has previously been addressed via a suitable modification of MEM [13] we propose here an alternate, and perhaps simpler, technique to couple, or glue, the physics back together through a lower-dimensional entity at the interface. For example, in 2D plane stress, a beam is used between the two sides of the interface. While [14] demonstrates beam to solid coupling we differ in that here the beam is oriented tangent to the surface instead of normal. This lower-dimensional entity "fills in the gaps" between the discrete models, acting as a mechanism to transfer information between the two meshes.



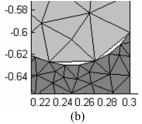


Figure 1: Two different forms of "non-conforming" meshes: (a) the mesh conforms to the CAD model (a line), but in (b) it does not conform to the CAD model (a circular arc).

Proposed Concept

The underlying concept behind the proposed approach is that since the discrete models do not represent the CAD models precisely, we fill these gaps (possible overlaps will be considered shortly) with a thin, possibly even zero thickness, lower-dimensional entity. This process in illustrated in Figure 2, where the outermost subfigures represent the two discrete models and the center subfigure illustrates the oriented thin region between them, together with the beam mesh. As this layer is thin it must be handled appropriately, e.g. as a beam in 2D. In particular, Euler-Bernoulli beam theory is invoked throughout this paper. Each parent mesh is glued to this lower-dimensional entity through Dirichlet coupling, in that each parent degree of freedom (DOF) is cast as a function of the lower-dimensional DOFs by simply evaluating the appropriate shape functions.

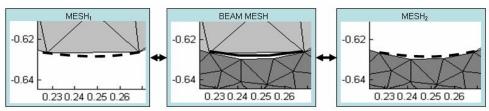


Figure 2: Example of two discrete models of a curved interface and their coupling to a beam mesh. In the subfigures the dashed line is the CAD model of the interface, while the solid lines are the beam mesh used during analysis.

As illustrated in Figure 2, the oriented beam region will, in general, be quite irregular and unfit for standard beam assembly where cross-sectional parameters must be explicitly determined. Instead, the recently developed dual-representation technique [15, 16] is used. For a thorough description of this method we refer the reader to [17] but for convenience we replicate the central idea here. For an Euler-Bernoulli beam oriented along a local x-axis (see Figure 3) the method is described below (taken from [17]):

$$u(x,y) \approx u_0(x) - yv_{0,x}$$

$$v(x,y) \approx v_0(x)$$
(1.1)

where $u_0(x) \& v_0(x)$ are the axial and bending displacements. The unknown displacements $u_0(x)$ and $v_0(x)$ are typically approximated via:

$$u_0(x) = N^u \hat{d}_0$$
 (1.2) $v_0(x) = N^v \hat{d}_0$

where:

$$N^{u} = \begin{cases} Q_{1}(x) & 0 & 0 & Q_{2}(x) & Q_{3}(x) & 0 & 0 \end{cases}$$

$$N^{v} = \begin{cases} 0 & H_{1}(x) & H_{2}(x) & 0 & 0 & H_{3}(x) & H_{4}(x) \end{cases}$$
(1.3)

where Q_i are quadratic shape functions, H_i are the cubic Hermitian shape functions, and \hat{d}_0 are the 7 degrees of freedom include 3 for axial stretching, and 4 for bending:

$$\hat{d}_0 = \left\{ \hat{u}_1 \quad \hat{v}_1 \quad \hat{\theta}_1 \quad \hat{u}_2 \quad \hat{u}_3 \quad \hat{v}_2 \quad \hat{\theta}_2 \right\} \tag{1.4}$$

Observe that the beam stress is given by:

$$\sigma_{xx} = E\left(u_{0,x} - yv_{0,xx}\right) \tag{1.5}$$

Further, it is easy to show that the stiffness matrix is given by:

$$K_{ij} = \int_{\Omega} E[(N_{i,x}^{u} - yN_{i,xx}^{v})(N_{j,x}^{u} - yN_{j,xx}^{v})]d\Omega$$
 (1.6)

i.e.,

$$K_{ij} = \int_{\Omega} E \begin{bmatrix} N_{i,x}^{u} N_{j,x}^{u} - y \left(N_{i,xx}^{v} N_{j,x}^{u} + N_{i,x}^{u} N_{j,xx}^{v} \right) \\ + y^{2} N_{i,xx}^{v} N_{j,xx}^{v} \end{bmatrix} d\Omega$$
(1.7)

At this point, the dual-representation method uses the divergence theorem to convert equation (1.7) to a boundary integral, leading to the following final definition of the stiffness matrix:

$$K_{ij} = \int_{\partial\Omega} E \begin{bmatrix} yN_{i,x}^{u}N_{j,x}^{u} \\ -\frac{y^{2}}{2}(N_{i,xx}^{v}N_{j,x}^{u} + N_{i,x}^{u}N_{j,xx}^{v}) \\ +\frac{y^{3}}{3}N_{i,xx}^{v}N_{j,xx}^{v} \end{bmatrix} n_{y}d\Gamma$$
(1.8)

Where n_{y} is the outward normal to the boundary

Effectively, this technique takes the definition of the internal energy of a beam, and converts it into a boundary integral so as to simultaneously capture the higher dimensional geometry and the lower-dimensional physics – hence the name dual-representations. It is interesting to note by using dual-representations, the beam mesh is not required to lie on the CAD model, but instead only needs to appropriately represent the beam region defined by the two discrete parent meshes.

In the case of overlapping mesh elements, equation (1.8) naturally computes a negative stiffness due to a negated outward normal. The negative stiffness is appropriate since the assembly of regions where overlaps occur are thrice accounted for, two positive and now one negative. The two positives come from the overlapping parent elements and the negative is from the inverted beam. This negative value effectively brings the total count to just one positive. The negative stiffness simply renders a (possibly) positive-definite matrix into an indefinite matrix.

Algorithm

In summary, the proposed technique can be broken down to the following steps for a 2D plane stress problem:

- 1) Assemble the plane stress stiffness matrices K_1^{ps} and K_2^{ps} for each of the two parent meshes.
- 2) Compute the boundary of the oriented region between the discrete models; see Figure 2 and Figure 3.
- 3) Define the particular physics of the beam region through a beam mesh. As previously mentioned, this mesh is not required to lie on the CAD model of the interface.
- 4) Compute the effective beam stiffness matrix K_b for this region via dual-representations. In the case that Euler-Bernoulli beam physics is assigned to the interface region equation (1.8) is appropriate.
- 5) Generate the Dirichlet coupling matrix, C, as follows:
 - a) For each node on both interface meshes:
 - i) Let the u, v degrees of freedom of this node in the beam coordinate system be \hat{u}, \hat{v} .
 - ii) Find the (x, y) coordinate of this node in the beam local coordinate system (see Figure 4).
 - iii) Evaluate $N^u, N^v, y \frac{dN^v}{dx}$ using equation (1.3) at the just computed (x, y) coordinate.
 - iv) Append the equations:

$$\hat{u} = \left[N^u - y \frac{dN^v}{dx} \right] \hat{d}_0$$

$$\hat{v} = N^v \hat{d}_0$$
 to C .

6) Assemble the system:

$$Ku = f$$

$$K = egin{bmatrix} ilde{K} & C^T \ C & 0 \end{bmatrix}, ilde{K} = egin{bmatrix} K_1^{ps} & 0 & 0 \ 0 & K_2^{ps} & 0 \ 0 & 0 & K_b \end{bmatrix}, f = egin{bmatrix} f_1^{ps} \ f_2^{ps} \ f_b \ 0 \end{bmatrix}$$

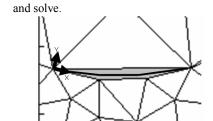
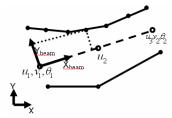


Figure 3: A beam (shaded region) with local x-direction of one beam element.



(1.9)

Figure 4: A portion of an interface mesh (solid lines), corresponding beam element (dashed line), beam DOF, and all attached nodes.

Examples

Here we demonstrate the concept through a 2D plane stress example that contains gaps and overlaps between the two discrete models. For all studies to follow, the material properties are: Young's Modulus is 2e11 [N/m²], and Poisson's Ratio is 0.33. Furthermore, the base CAD model, together with the boundary conditions, is illustrated in Figure 5. The interface is comprised of two circular arcs and a line segment that is tangent to the arcs. This provides a region with overlaps (Figure 6a), a region where the beam thickness is zero (Figure 6b), and a region with gaps (Figure 6c). In addition, the *exact solution* is always taken to be that of a highly refined fully conforming finite element model.

In the first example, we assign the same 'mesh-size' to the two domains, i.e., the meshes conform. Further, the beam is also discretized with the same mesh-size. Figure 7 shows the resulting error in the energy norm versus the global mesh size. We observe the expected drop in error confirming that the proposed method recovers the 'true' solution in the case of a conforming mesh.

The next example investigates the generality of the proposed method. The mesh parameters are held constant through each test where a mesh-size of 0.03 [m] is assigned to the upper sub-domain, and 0.017 [m] is assigned to the lower sub-domain. Table 1 shows various CAD models used at the interface during the experiment; the resulting mesh-

models have significant overlaps and gaps (not illustrated due to lack of space). The predicted maximum x-displacement is summarized in Table 1. As the results indicate, the method is insensitive to various pathologies that may arise, and can handle significant overlaps and gaps with relative ease.

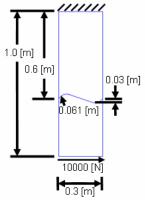


Figure 5: Base geometry with interface, dimensions, and boundary conditions.

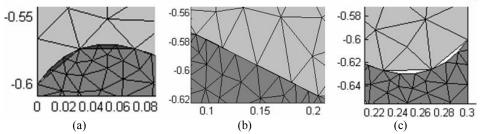


Figure 6: The interface with: (a) overlapping elements, (b) classic "non-conforming" mesh, and (c) gaps.

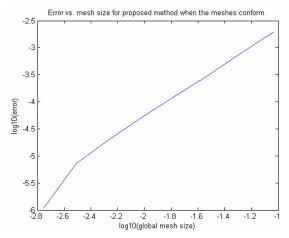


Figure 7: Error in energy norm versus global mesh size for proposed method.

Table 1: Max x-displacement for various interface geometries

Interface curve	Max(u) [um]
	2.37092
	2.37093
	2.37096
	2.37101
	2.37101
	2.37090
	2.37089
	2.37085
	2.37085
	2.37083

Conclusions

We have proposed here a simple method to couple non-conforming meshes using a lower-dimensional entity. As supported by theory and experiments, the proposed method can handle both gaps and overlaps in adjacent discrete models with relative ease.

References

- 1. Smith, B., Bjorstad, P., Gropp, W., *Domain Decomposition*. 1996: Cambridge University Press.
- Quarteroni, A., Valli, A., Domain Decomposition Methods for Partial Differential Equations. 1999, New York: Oxford Science Publications.
- 3. Belgacem, F.B., *The Mortar finite element method with Lagrange multipliers*. Numerische Mathematik, 1999. **84**(2): p. 173-197.
- 4. Cai, X.-c., M. Dryja, and M. Sarkis, Overlapping Non-Matching Grid Mortar Element Methods For Elliptic Problems. 1998.
- 5. Wohlmuth, B.I., A Mortar Finite Element Method Using Dual Spaces for the Lagrange Multiplier http://dx.doi.org/10.1137/S0036142999350929 SIAM J. Numer. Anal., 2000 38 (3): p. 989-1012
- 6. Zienkiewicz, O.C., Taylor, R. L, Zhu, J. Z., *The Finite Element Method: Its Basis and Fundamentals*. 6th Edition ed. 2005: Elsevier Butterworth Heinemann.
- 7. Dohrmann, C.R., S.W. Key, and M.W. Heinstein, *Methods for connecting dissimilar three-dimensional finite element meshes*. International Journal for Numerical Methods in Engineering, 2000. **47**(5): p. 1057-1080.
- 8. Japhet, C., Y. Maday, and F. Nataf, *A new Cement to Glue non-conforming Grids with Robin interface conditions: the finite element case.* 2007.
- 9. Pantano, A. and R.C. Averill, *A penalty-based finite element interface technology*. Computers & Structures, 2002. **80**(22): p. 1725-1748.
- 10. Hu, Q., A regularized domain decomposition method with Lagrange multiplier. Advances in Computational Mathematics, 2007. **26**(4): p. 367-401.
- Lacour, C. and Y. Maday, Two different approaches for matching nonconforming grids: the mortar element method and the FETI method. 1997, HAL - CCSD L2 - HAL: http://hal.archives-ouvertes.fr/hal-00369517/en/
- Arbogast, T. and I. Yotov, A non-mortar mixed finite element method for elliptic problems on non-matching multiblock grids. Computer Methods in Applied Mechanics and Engineering Containing papers presented at the Symposium on Advances in Computational Mechanics, 1997. 149(1-4): p. 255-265.
- 13. Flemisch, B., M.A. Puso, and B.I. Wohlmuth, *A new dual mortar method for curved interfaces: 2D elasticity*. International Journal for Numerical Methods in Engineering, 2005. **63**(6): p. 813-832.
- 14. Shim, K.W., Monaghan, D. J., Armstrong, C. G., *Mixed Dimensional Coupling in Finite Element Stress Analysis*. Engineering with Computers, 2002. **18**(3): p. 241-252.
- 15. Jorabchi, K., Danczyk, J., Suresh, K., Efficient and automated analysis of potentially slender structures. Journal of Computing and Information Science in Engineering, 2009. 9(4): p. 041001 (9 pages).
- Mishra, V. and K. Suresh. Efficient Analysis of 3-D Plates via Algebraic Reduction. in Proceedings of the ASME 2009 International Design Engineering Technical Conferences & Computers and Information in Engineering Conference. Aug/Sept, 2009. San Diego, CA.
- 17. Samad, W.e. and K. Suresh, *CAD-integrated analysis of 3-D beams: a surface-integration approach.* Engineering with Computers.